

Report

Cardio-eigenoscopy: significance of this new method in prognosis of risks of fatal arrhythmia progression in AMI patients

Dmitry V. Issakevich¹, Vladimir V. Chepenko^{1*},
Mikhail Y. Rudenko², Konstantine K. Mamberger²

¹ Vladimir State University, Faculty of Applied Mathematics and Physics, 600026, Russia, Vladimir, Stroiteley av. 3/7

² Russian New University, 105005, Russia, Moscow, 22 Radio St.

* Corresponding author: E-mail: chepenko.vladimir.49@mail.ru

Submitted: 28 March 2013

Accepted: 20 April 2013

Published online: 30 May 2013

Abstract

The aim of the study was to evaluate the significance of cardio-eigenoscopy method for the prognosis of risks of fatal arrhythmia (the primary and secondary VF) progression in AMI individuals. The study was performed with the use of the PC-assisted hemodynamic analyzer Cardiocode. The cardio-eigenoscopy was developed as a methodology that is capable of presenting all ECG changes in the basis of eigenvectors of a covariance matrix of ECG amplitudes and providing an analysis of a spectrum of eigenvalues. The ECG analysis software is implemented as a real-time monitoring of a set of parameters that makes possible to evaluate the therapy effectiveness.

The cardio-eigenoscopy method is capable of assessing the risk of progression of fatal arrhythmia events in MI patients. The major markers of the possible progression of fatal arrhythmia were identified. The cardio-eigenoscopy provided the maximum expressibility of an ECG curve at any specified EVE values.

Keywords

Arrhythmia • Cardiovascular system • ECG • Cardio-eigenoscopy • Myocardial infarction

Imprint

Dmitry V. Issakevich, Vladimir V. Chepenko, Mikhail Y. Rudenko, Konstantine K.Mamberger. Cardio-eigenoscopy: significance of this new method in prognosis of risks of fatal arrhythmia progression in AMI patients; *Cardiometry*; No.2; May 2013; p.104-123; doi: 10.12710/cardiometry.2013.2.104123

Available from:

<http://www.cardiometry.net/issues/no2-may-2013/cardio-eigenoscopy.pdf>

Introduction

Cardiac insufficiency (CI) is a clinical manifestation of various cardiac diseases. This is a condition when compensatory mechanisms of the cardiovascular system are no longer incapable of maintaining the normal homeostasis. Nowadays there are more than 22 million CI patients throughout the world. According to different estimations, a sudden stoppage of blood circulation is annually reported for 200 000 to 450 000 subjects in the United States, and it is the cause of 95% of the cases of sudden cardiac death (SCD). In the developed European countries sudden cardiac death accounts for 2500 deaths per day, with only 2% to 5% of the SCD statistics referred to patients' stay registered upon their admission to medical institutions. The world-covering predicted SCD rate is about 3 000 000 deaths per year with the 1.0% chance of survival only. The chance of a successful outcome upon intensive care does not exceed 5% in the economically developed countries. 40% of sudden cardiac death cases cannot be identified at all, or are reported as occurred in sleep. It should be noted that 80% of the SCD cases occur at home or other places of permanent residence. The well-known Framingham heart study (1970) has shown that the survival coefficient with the initial CI diagnosis accounts for 62% of males and 42% of females. The share of the SCD cases in the total mortality rate was 40% to 50% [1, 2].

The main nosological cause of SCD progression is ischemic heart disease (IHD) that is reported in 80% to 85% of the SCD cases, including more than 65% which are connected with an acute stoppage of blood flow in the coronary arteries. Further 5% to 10% of the SCD cases are caused by dilated cardiomyopathy (DCM), and the remaining 5% to 10% of the SCD cases are induced by other cardiac diseases. In the circumstances, arrhythmias are treated to be the direct mechanism of the circulation stoppage, with 90% of ventricular tachyarrhythmias among them. Electromechanical dissociation and bradyarrhythmia lead to the circulation stop in 10% of all SCD cases.

In accordance with the modern concepts, etiology and pathogenesis of ventricular arrhythmias (VA) in IHD subjects imply that there is an interaction of numerous factors we have to deal with, which are as follows: structural cardiac changes [3,4,5], myocardial electrical instability (MEI), neurohumoral mechanisms [6,7], circadian biorhythms [8,9] and genetic defects [10,11].

It is reported that about 20% of the patients survived upon intensive care show no signs of myocardial ischemia, but almost without exception they have an apparent ventricular dysfunction that takes place after previous myocardial infarctions. With respect to these patients, it should be noted that the predictor of their mortality in general, including the SCD mortality, is a reduction in the pumping function in the cardiovascular performance, but not

the accompanying arrhythmias. In case of insufficient pumping function of the left ventricle, extrasystole being correlated with the degree of the LV function reduction is observed in 80% of the cases for the said patients.

A reduced cardiac output and a nonsustained ventricular tachycardia (VT) recorded by Holter-monitoring ECG and identified during an electrophysiological study of post-AMI patients remain currently to be used as the main prognostic markers of a high risk of the SCD [12,13]. One of the latest studies in subjects with Implantable Cardioverter Defibrillators (ICD) demonstrates that sudden occurrence of the ventricular tachycardia (VT) or ventricular fibrillation (VF), as a rule, is found in patients showing an unchanged cardiac output; a gradual growth of ventricular ectopic activity accompanied by the lowered contractility is observed in the above patients before the VT or VF attacks. The lowered left ventricular contractility increases the SCD risk not only for the IHD subjects, but also for patients suffering from other heart diseases [14,15]. An apparent atherosclerotic narrowing (over 50%) of the coronary arteries is found in 90% of the SCD cases. The degree of damage of the coronary arteries plays an important role in VA and SCD progression [10,11]. According to a great number of clinical investigations, both symptom-accompanied and symptom-free myocardial ischemia types are considered as an informative SCD risk marker for the patients suffering from different IHD forms [16,17,18]. Known is the so-called SCD triangle of IHD patients which is constructed by myocardial ischemia, myocardial electrical instability (MEI) and left ventricular dysfunction [19]. It should be noted that the most unfavorable combination is produced by two SCD risk factors which are as follows: the frequent ventricular extrasystole and the left ventricular dysfunction with a reduced cardiac output < 40 %. According to the GISSI-2 research studies, under the said conditions, a 16-fold increase in the risk of sudden arrhythmic death is reported [3]. A life threatening VA (stable VT, VF) occurs when a combination of several MEI predisposing factors appears which are as follows: a substrate (a structural disease of the heart) modulating the dysfunction of the vegetative nervous system and some VA triggering factors. The morphological substrate producing the post-MI inhomogeneity of impulse conductivity is a myocardial area which is a boundary area being located in the vicinity of necrotic tissues of myocardium and which is formed by interlaced islets made of viable myocardial fibers and conjunctive tissue. The impulse conductivity path is extended there due to conjunctive tissue islets hindering the cardiac impulse traveling, and the conductivity speed falls due to disorders in muscle fibre parallel orientation. Besides, known are some other SCD risk factors, in particular, a disturbance in the vegetative regulation of the heart with the dominance of the sympathetic activity. The most important marker of this abnormality is a reduced variability of sinus rhythm [20], along with an extended Q-T interval and a dispersion

of the latter [21,22]. The reduced rhythm variability and the extended Q-T interval are deemed to be supplementary MEI indicators [21]. An apparent left ventricular hypertrophy, especially in subjects suffering from arterial hypertension [23,24,25,26,27] and hypertrophic cardiomyopathy [28,29], is considered to be one of the SCD risk factors. The discussion on what antecedents of the VF are available is still in progress, and so far there is no consensus of opinion among the experts. The commonly accepted risk factors of life-threatening VA progression for IHD patients do not show the proper sensitivity and the specificity, and life sets us a challenge to find some absolutely new MEI markers [27,28].

The cardio-eigenoscopy method makes possible to provide an analysis of real-time cardiac signal shape changes with an assessment of risks of progression of fatal arrhythmias.

Materials and methods

The aim of our study was to evaluate the significance of cardio-eigenoscopy method for the prognosis of risks of fatal arrhythmia (the primary and secondary VF) progression in AMI individuals. 56 MI-diagnosis individuals with different MI localizations, on hospital days 1 to 10, were covered by the study. The test cohort included 13, 6% of females and 86,4% of males. The mean age was 63 years. Group 1 comprised 42 patients survived. Group 2 comprised 14 subjects with lethal outcome. The study was conducted on hospital days 1, 3, 5 and 7-9 in the dynamics.

The study was performed with the use of the PC-assisted hemodynamic analyzer Cardiocode. The cardio-eigenoscopy has been developed as a methodology that is capable of presenting all ECG changes in the basis of eigenvectors of a covariance matrix of ECG amplitudes and providing an analysis of a spectrum of eigenvalues. The ECG analysis software is implemented as a real-time monitoring of a set of parameters that makes possible to evaluate the therapy effectiveness.

In the offered methodology, a covariance matrix is computed with the utilization of a matrix of an ensemble of cardiac oscillations. The ensemble is created by a segment of a cardiac signal which refers to several tens of cardiac contractions. Every ensemble element represents a portion of a signal with a certain length, containing the respective signal generated by a single cardiac contraction.

Processed are the successive discretized and digitalized cardiac signal segments which have an N discrete length and which comprise several tens of the cardiac oscillations, as mentioned above. The signal in each segment is specified by a series of discrete counts $S_i, i = \overline{1:N}$. An example of a cardiac signal with the dominance of peaks is illustrated in Fig.1.a herein. This signal is of infrequent occurrence. Fig.1.b displays another cardiac signal which is relevant to

fibrillation (a coma patient). As the figure suggests, no dominance of peaks is available in the case illustrated in the said figure.

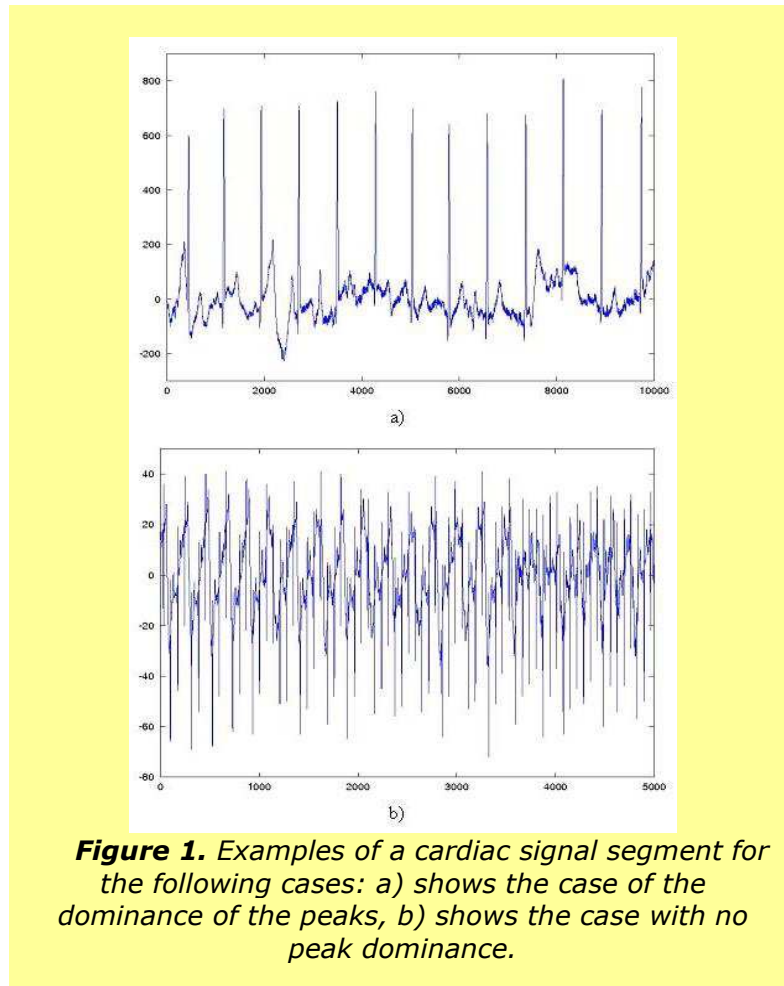
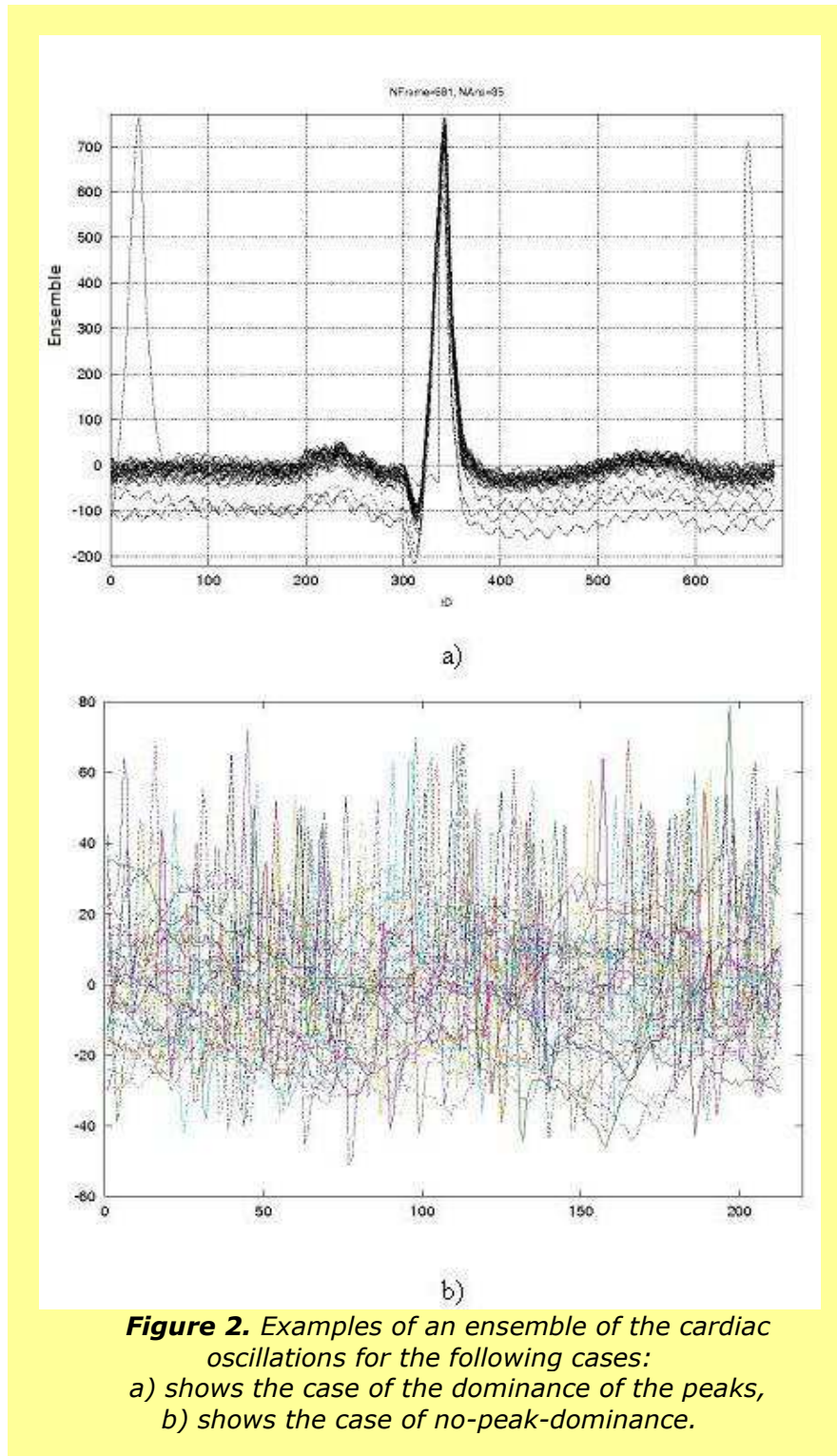


Figure 1. Examples of a cardiac signal segment for the following cases: a) shows the case of the dominance of the peaks, b) shows the case with no peak dominance.

Each of the successive length part of the N length is centered and brought to "the normal form" (with positive peaks if they dominate). If we deal with the peak dominance (that is determined by the R wave amplitude), locations of the peaks and an averaged period of their recurrence $T_{cp,N}$ are identified, and then the respective ensemble of the cardiac oscillations is created. If no dominance of the peaks is observed, an averaged period is identified immediately, and thereafter an ensemble is created. Each element of such an ensemble represents a matrix row describing a separate segment of a cardiac signal on an interval which is equal to the averaged period. In case of the dominance of the peaks, the cardiac oscillation peak is located in the center of the above matrix row, and the full length of the matrix row is equal to the discrete value of the averaged period $T_{cp,N}$. Fig.2.a offers us an illustration of

such ensemble for the peak dominance case, and Fig.2.b indicates another case, when no peak dominance is observed.



The ensemble is a rectangular matrix $T_{K \times T_{cp,N}}$ with a dimension of $K \times T_{cp,N}$, where K is the number of elements of the ensemble that is equal to the number of the cardiac oscillation integers with a dimension of $T_{cp,N}$ which are presented along the analysis interval N .

With the use of the matrix $T_{K \times T_{cp,N}}$ a covariance matrix of the cardiac oscillations is calculated from a formula as given below:

$$K_{T_{cp,N} \times T_{cp,N}} = \frac{T_{K \times T_{cp,N}} \cdot T_{K \times T_{cp,N}}'}{K - 1}, \quad (1)$$

where $(...)'$ is the matrix transpose.

For the covariance matrix (1) we can find the eigenvectors (EVEs) and the eigenvalues (EVAs) which satisfy the relation as follows:

$$K_{T_{cp,N} \times T_{cp,N}} \cdot \psi_i = \lambda_i \cdot \psi_i, \quad i = \overline{1: T_{cp,N}}. \quad (2)$$

The dimensionality of the covariance matrix for the case of cardiac signal discretization with the 10^{-3} second period is usually less than 700. The time required for the calculation of the covariance matrix described by the relation (1) for $K \leq 50$ and the calculation of the matrix EVE and EVA for $T_{cp,N} \leq 700$, using standard computation tools, is 1 to 5 seconds. Therefore, it is possible to trace the EVEs and the EVAs of the covariance matrix under the real-time conditions.

An averaged energy of the signal observed on the interval $T_{cp,N}$ is described by the relation given below:

$$\tilde{\mathfrak{E}} = \sum_{i=1}^{T_{cp,N}} \lambda_i. \quad (3)$$

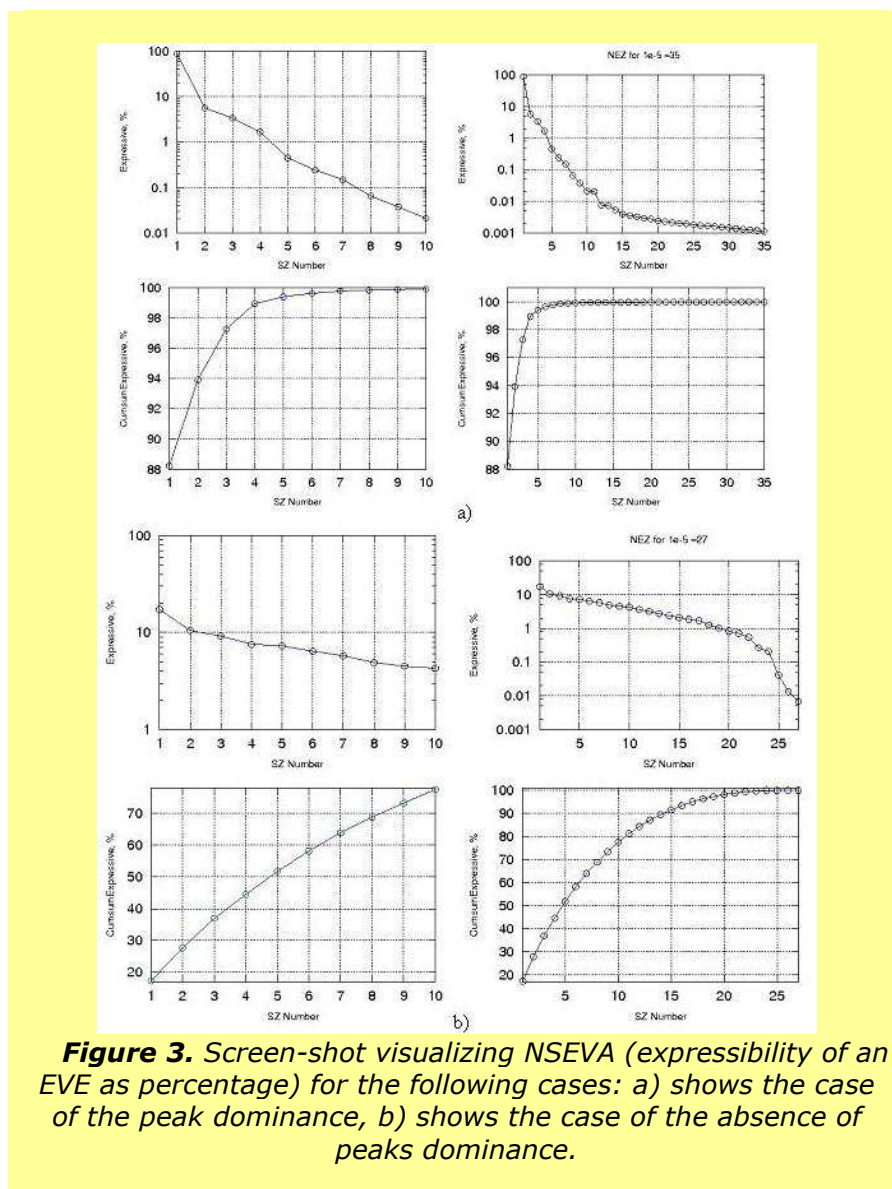
This implies that the series

$$\tilde{\mathfrak{E}}_{OTH}^{(i)} = \frac{\lambda_i}{\sum_{i=1}^{T_{cp,N}} \lambda_i}, \quad (4)$$

which will be further referred to as the normalized spectrum of eigenvalues (NSEVA) determines the relative share in the average energy (3) that belongs to the corresponding EVE. Further, as it is the case with [1], the NSEVA will be arranged in a descending order. Since every NSEVA parameter expresses the relevant information on the energy share which is "credited" to the relative EVE, the NSEVA value of the respective EVE will be referred to as the

expressibility of the said EVE. The expressibility can be evaluated in percent, so that the total expressibility of all EVEs is 100%. The higher the expressibility of an EVE is, the more information it contains and the greater energy the respective cardiac signal component possesses.

It can be shown that the NSEVA for the covariance matrix (1) constructed with the use of $T_{K \times T_{cp,N}}$ possesses such a number of non-zero EVAs that is equal to K . A screen-short presented in Fig.3.a herein (s. top right window) demonstrates the typical NSEVA (4) constructed for the case $K = 35$ and $T_{cp,N} = 680$. As will be seen from the plot in the above window, the first 35 NSEVA values only exceed the level of 10^{-5} .



But even the above mentioned number of the NSEVA values is redundant for the analysis. The top left window in a screen-shot presented in Fig.3.a displays the first 10 NSEVA values, where only the 4 of them demonstrate their expressibility exceeding 1%, and only the 7 of them show their expressibility higher than 0.1%. Therefore, it may be concluded that for the purposes of diagnostics it is quite sufficient to visualize the first 10 of the NSEVA values. The bottom windows in the screen-shot in Fig.3.a contain some plots of the cumulative expressibility. Every plotted point is the sum of the number of the first NSEVA values specified on the abscissa. So, the bottom left plot indicates that the first 4 NSEVA values provide their cumulative expressibility (the credited averaged energy) at a level of 99%. This parameter is typical for the healthy heart.

In case when fibrillation is available, we deal with another condition: the expressibility of the first EVE is considerably reduced, while the expressibility both of the first and the second EVE becomes comparable. It is displayed in the respective screen-short given in Fig.3.b. In case of the absence of the peak dominance, the first 10 NSEVA values might be insufficient for the analysis of the expressibility. Therefore, it should be recommended to utilize all NSEVA parameters higher than 10^{-5} .

A screen-shot shown in Fig.4.b offers a typical example of the first four EVEs for the no-peak-dominance case.

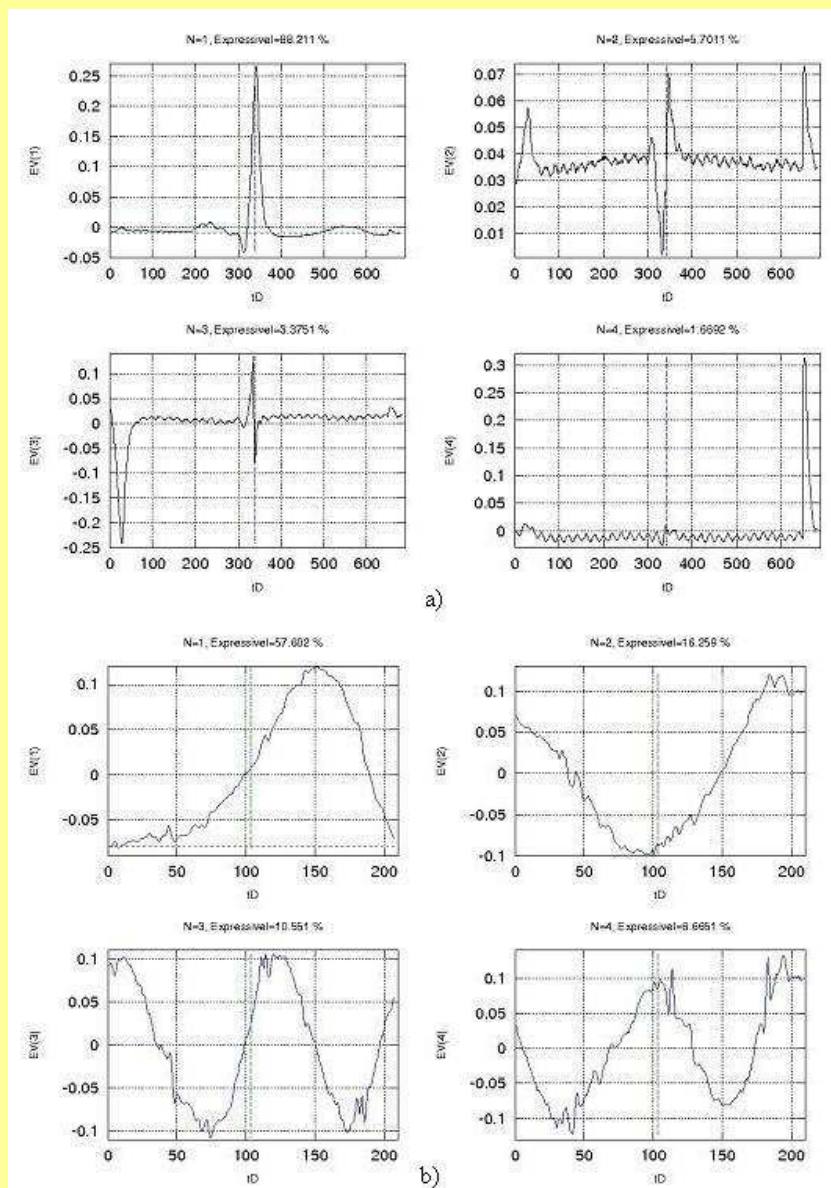
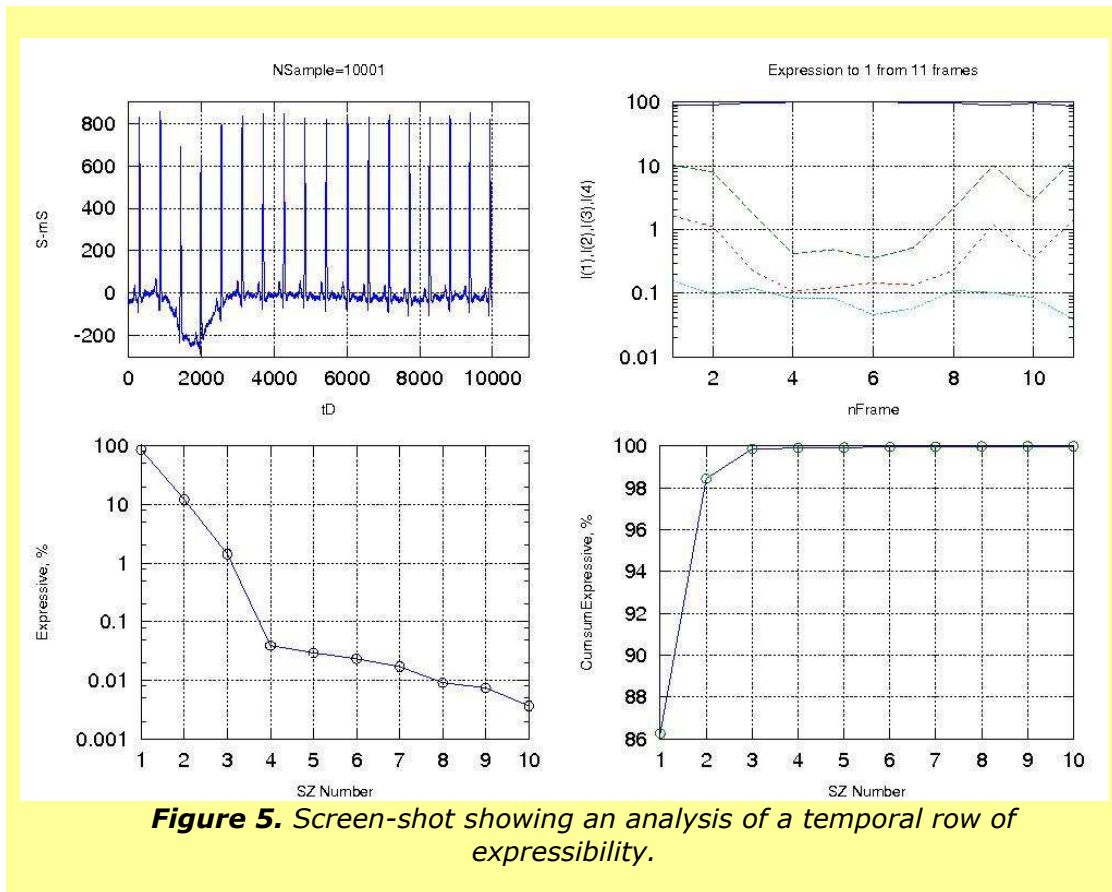


Figure 4. Screen-shot visualizing the first four eigenvectors for the following cases: the peak dominance case is illustrated in a), and the no-peak-dominance case is indicated in b). The windows above the plots indicate the No. of each EVE and the respective expressibility in %.

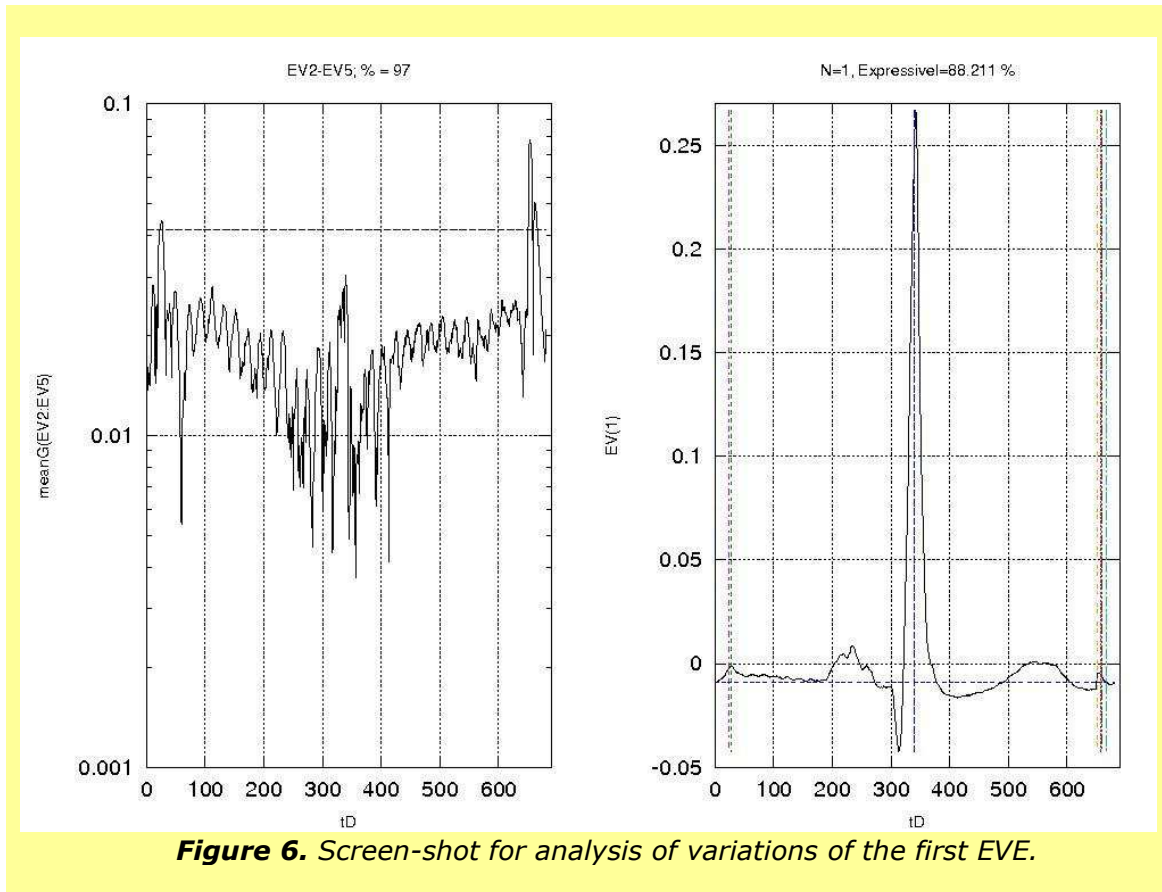
The EVE expressibility may vary with time. A screen-shot shown in Fig.5 depicts a plot in the top right window to demonstrate how the expressibility of the first four EVEs is varying throughout 11 analysis intervals; the left top window presents the initial cardiac signal on the last analysis interval, and the bottom windows display the first 10 NSEVA values for the last analysis interval (left) and the cumulative NSEVA for the same analysis interval (right).



The NSEVA analysis suggests that it is reasonable to analyze the first EVEs only, which demonstrate their highest expressibility. A screen-shot in Fig.4.a gives us an illustration of the first four EVEs for a specified interval of the analysis used for the peak-dominance case. It is evident from the figures that the first EVE shows actually the maximum expressibility (over 88%). The other three EVEs might have significance to be applied to the analysis in some specific cases only. For instance, it might be done when we deal with a weakened level of the cardiac signal being below the harmonic noise level, the first (and eventually the second) EVE would contain some noise, then the next EVEs would express the cardiac signal.

The EVEs given under Nos. 2 to 4 in the above figure are less expressible than the first EVE, and, as a rule, they contain information on noises affecting the cardiac signal and the

fluctuations of the latter. To identify zones of instability of the cardiac oscillations, an approach is offered as described below. For the EVE modules under Nos. 2-4, the geometric mean should be found (an example is shown in the left window on a screen-shot in Fig.6).



The top right window (Fig.6) shows the first EVE with instability areas indicated (marked with vertical viewers). In order to identify instability zones, the geometric mean value plot is used, in this case for the 2-5 EVE modules (given in the left window). A quantile in the specified order is computed from this geometric mean value plot (left side indication: a quantile of the 97% level), thereafter areas, where a quantile is exceeded by the geometric mean values, are computed which are indicated as instability zones in the right window.

On those time intervals where all above mentioned EVEs (under Nos. 2-4) show their high values, the geometric mean is also high. For the geometric mean, a quantile according to a specified order can be computed (the said figure shows an example for the percentile $X_{0.97}$), and the time interval boundaries, where the geometric mean exceeds the quantile, can be determined. It is precisely these boundaries that clearly identify the instability zones of the cardiac oscillations and that can be visualized by plotting of the first EVE, as it is illustrated in

the right window in the screen-shot in Fig.6 herein. Such way of identifying the instable zones of the expressibility considerably facilitates the diagnostics procedure.

Finally, the obtained EVEs can be used to reconstruct or restore cardiac oscillations. In this case we use a formula as follows

$$T_{\text{recon},L} = T_{K,T_{cp},N} \cdot \psi_{1:L} \cdot \psi'_{1:L} , \quad (5)$$

where

$T_{\text{recon},L}$ is an ensemble consisted of the K cardiac oscillations reconstructed or restored with L EVE,

$T_{K,T_{cp},N}$ is an initial ensemble of the cardiac oscillations to construct or to restore the EVE,

$\psi_{1:L}$ is the EVE matrix utilized for the said reconstruction or restoration (the EVEs are written as columns in this matrix).

Fig.7 and 8 illustrate an example of the reconstruction or restoration with the use of the formula (5) for the cases $L = 4$ and $L = 2$, accordingly.

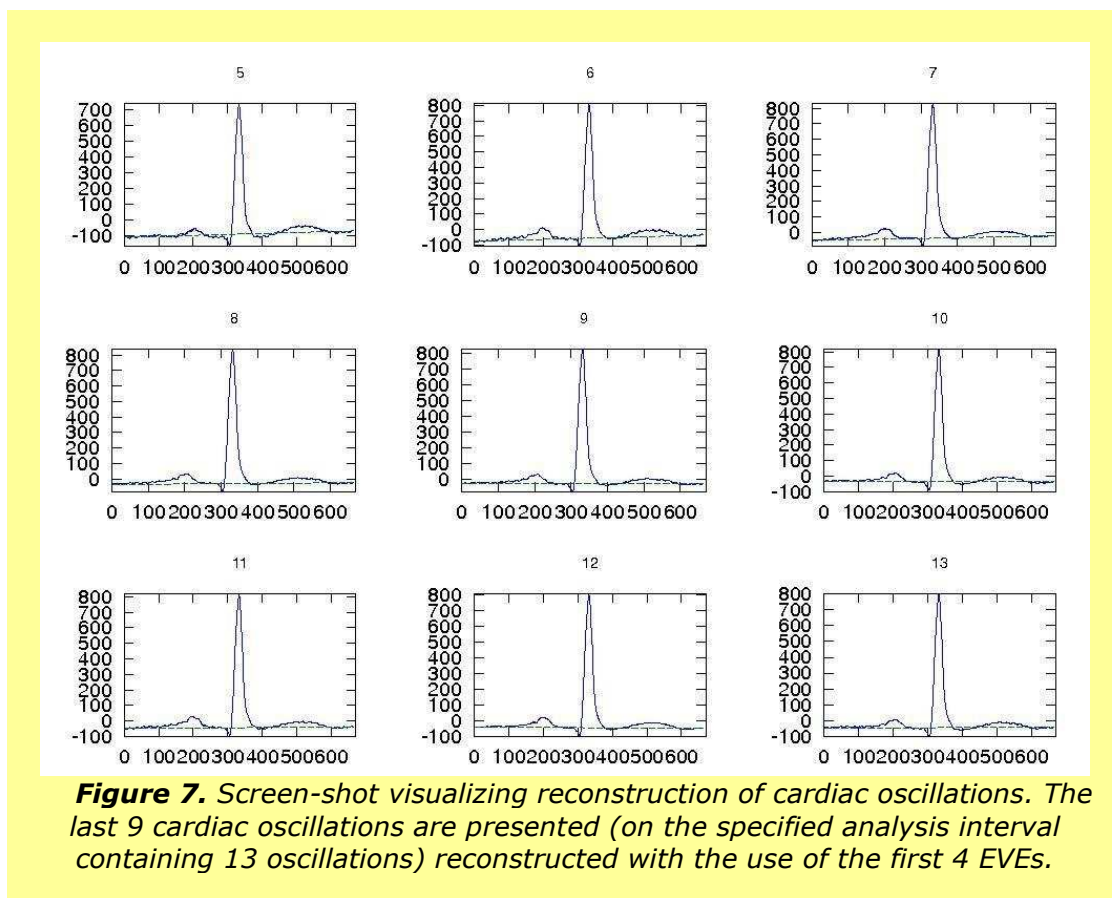
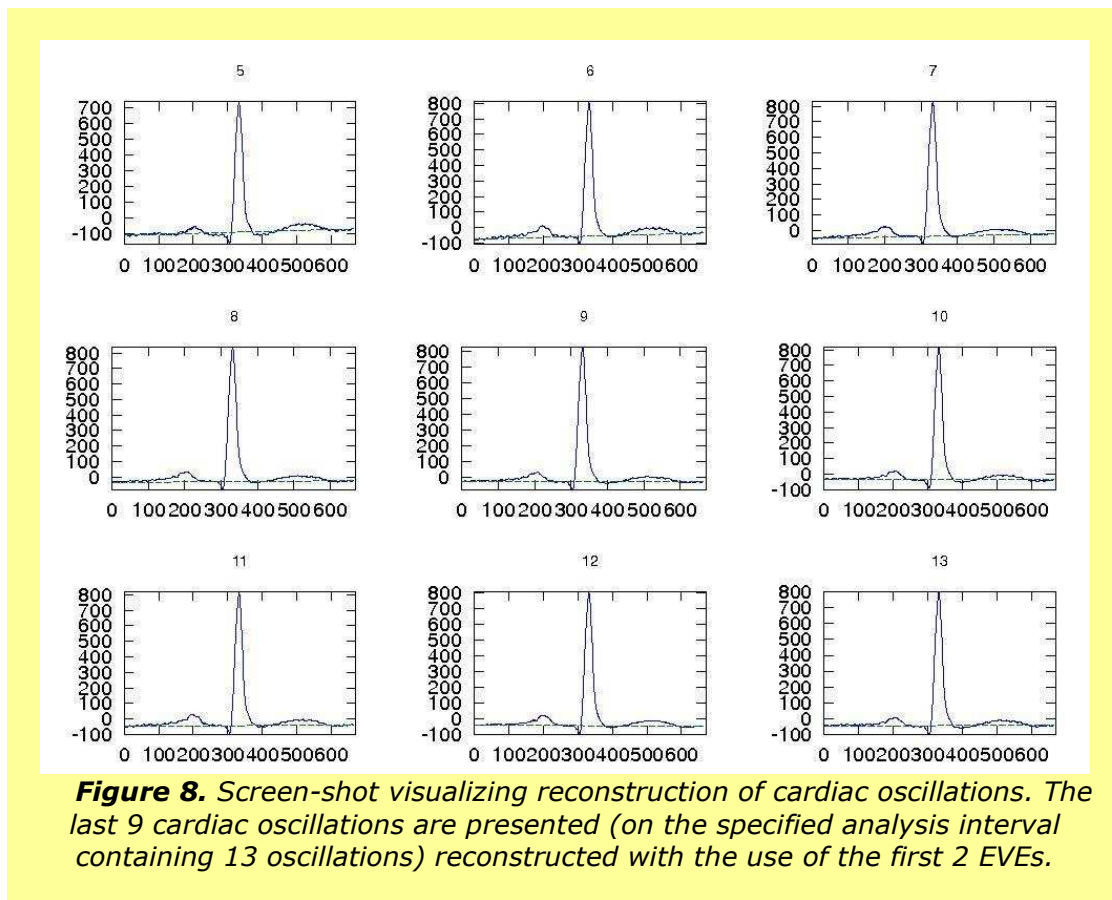


Figure 7. Screen-shot visualizing reconstruction of cardiac oscillations. The last 9 cardiac oscillations are presented (on the specified analysis interval containing 13 oscillations) reconstructed with the use of the first 4 EVEs.



It should be noted that there are several options how to provide the proper visualization of the data produced by the analysis performed by the hemodynamic analyzer Cardiocode. The most effective way of the visualization is an application of a two-window visualization interface that is illustrated in Fig.9 and 10 showing two cases described earlier: the peak-dominance case and the no-peak-dominance case.

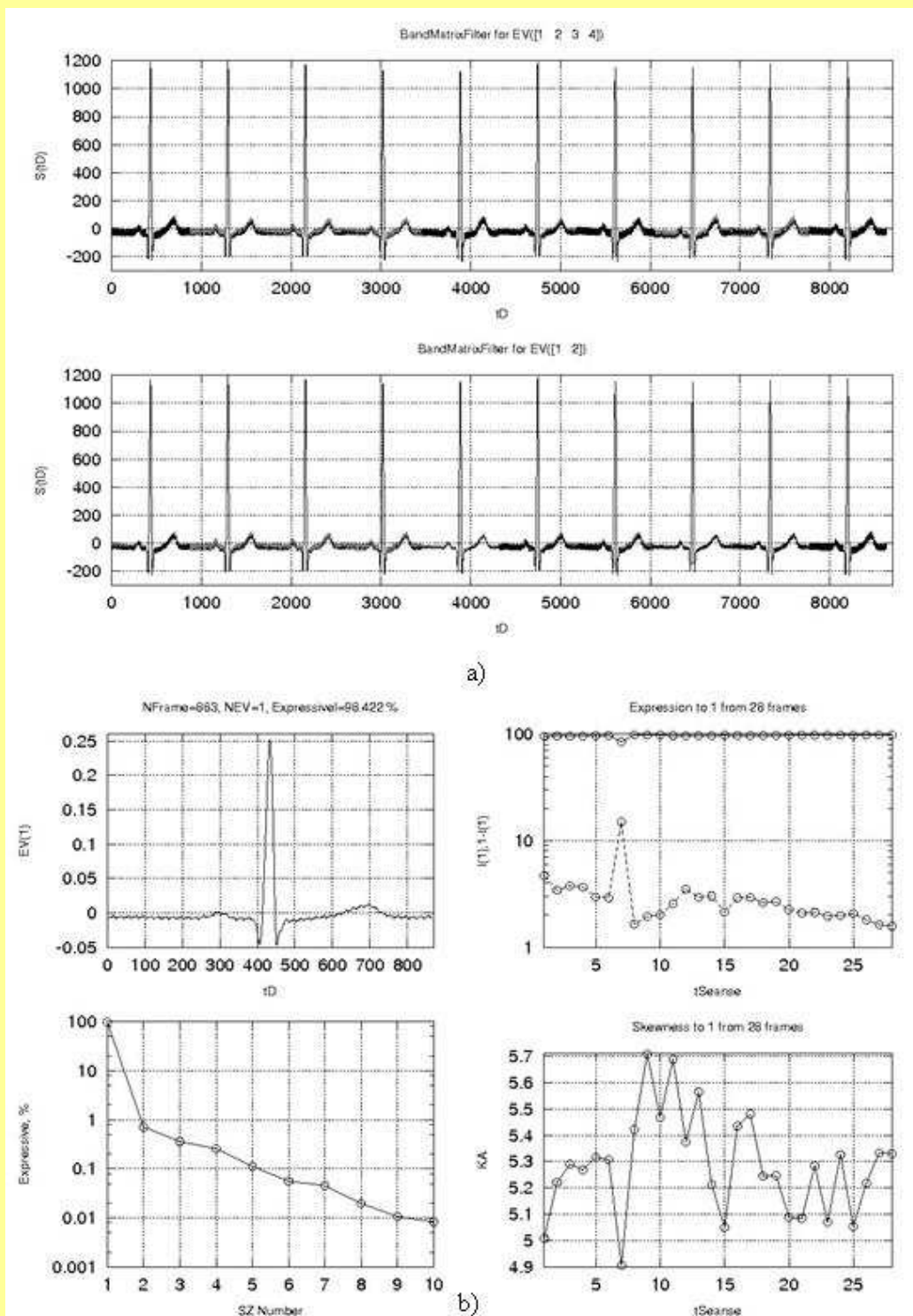


Figure 9. Analyzer screen-shots displaying a cardiac signal with the peak dominance.

The top left window indicates the first EVE (Fig.9 a). The bottom left window shows EVE expressibility. The top right window shows temporal rows of expressibility of the first EVE (the top plot) and cumulative expressibility of the other EVEs (the lower plot). The bottom right window indicates an asymmetry coefficient temporal row.

The top window in Fig.9.b) displays a cardiac signal on the analysis interval reconstructed with the first four EVEs. The bottom window is a cardiac signal on the analysis interval reconstructed with the first two EVEs.

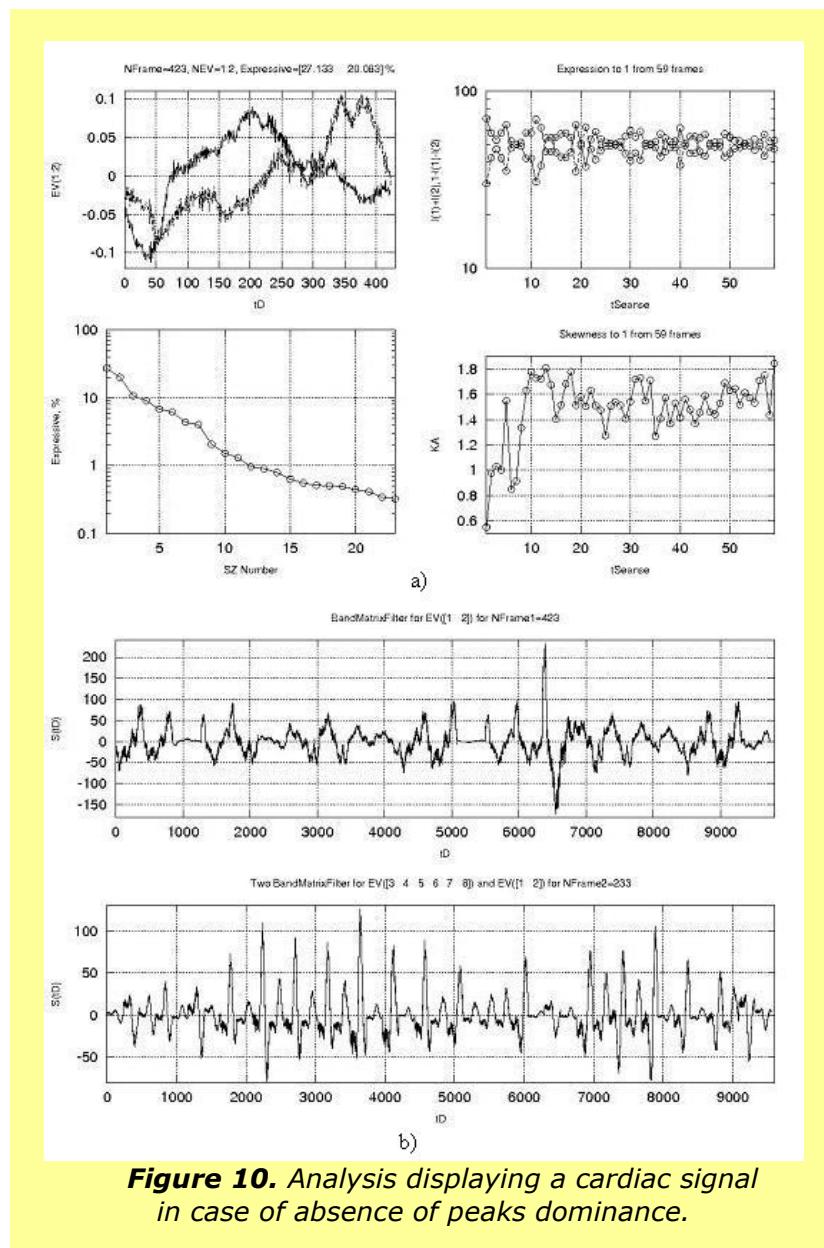


Figure 10. Analysis displaying a cardiac signal in case of absence of peaks dominance.

The first screen-shot is given in Fig.10.a). The top left window indicates the first and the second EVE, respectively. The bottom left window shows expressibility. The top right window indicates temporal rows of expressibility of the first EVE (the top plot) and cumulative expressibility of the other EVEs (the lower plot). The bottom right window indicates an asymmetry coefficient temporal row.

The second screen-shot is given in Fig.10.b). The top window displays a cardiac signal on the analysis interval reconstructed with the first two EVEs. The bottom window indicates the following procedure: the components corresponding to the first four EVEs are excluded from the cardiac signal, next an EVE basis is constructed for the signal newly produced, and by using the first two of the newly constructed EVEs a high-frequency component is identified.

As indicated in Fig.10 b), if necessary, the reconstruction or the restoration of cardiac signal components can be undertaken many times. A screen-shot presented in Fig.10 b) demonstrates the reconstructed cardiac signal (top window) upon the completed reconstruction procedure which is as follows: initially, the first 4 components of the signal are removed, thereafter, for the remainder an ensemble is created once again, on the basis of which new EVEs are obtained, and with the use of the first two newly produced EVEs the reconstruction is performed.

The cardiac oscillation ensemble for the cases of the peak dominance and no-peak-dominance are created, as discussed earlier, on an interval equal to the averaged period of the cardiac oscillations (that corresponds to the heart rate). But there are differing algorithms which are utilized for measuring of the averaged period in the above mentioned cases. The above mentioned hemodynamic analyzer is capable of automatically differentiating the type of the signal to be analyzed on any specified interval of the analysis.

According to the conducted surveys, the best quality in the proper differentiation of the cases of the peak dominance and no-peak-dominance is provided with the use of the criterion applying the asymmetry coefficient γ_1 , calculated by a standard formula as follows:

$$\gamma_1 = \frac{\frac{1}{N} \sum_{i=1}^N (S_i - m_x)^3}{\sigma^3}, \text{ where } m_x = \frac{1}{N} \sum_{i=1}^N S_i \text{ is the sample average, } \sigma^2 = \frac{1}{(N-1)} \sum_{i=1}^N (S_i - m_x)^2$$

is the sample dispersion, $S_i, \overline{1:N}$ is the cardiac signal sampling on the analysis interval.

In this case, the best threshold value of the dominance criterion employing the asymmetry coefficient is value 2. Therefore, it should be offered to apply to the analysis performed by the hemodynamic analyzer the following decisive rule:

if $\gamma_1 \geq 2$, the dominance of peaks is available,

if $\gamma_1 < 2$, the dominance of peaks is not available.

We dwell on the issue on how the ensemble of the cardiac oscillations is created by the Cardiocode device that is used to calculate the respective covariance matrix including the EVEs and EVAs of the latter. The selection of an averaged period to be used as an interval in the analysis (covering both cases: with peak dominance and no-peak-dominance) has the advantage (as the special surveys has demonstrated) that, under such conditions, the EVE maximum expressibility is observed. It is applicable to a greater extent to the case when the dominance of the peaks is available.

Conclusions

The cardio-eigenoscopy method is capable of assessing the risk of progression of fatal arrhythmia events in MI patients within 6 to 7 hospital hours by automatic analyzing the degree of variation of the specific ECG records in 97,5% of cases (showing the sensitivity of 88% and the specificity of 93,6%).

It has been found that the major markers of the possible progression of fatal arrhythmia are as follows: a share of the first vector was reported to be reduced to 80% and an ECG asymmetry coefficient was recorded to fall to 2,2. So, it should be noted that the cardio-eigenoscopy provides the maximum expressibility of an ECG curve at any specified EVE values. To provide an efficient analysis, it would suffice to use no more than 3 eigenvectors.

Statement on ethical issues

Research involving people and/or animals is in full compliance with current national and international ethical standards.

Author contributions

All authors prepared the manuscript and read the ICMJE criteria for authorship, V.V.C. drafted the manuscript. All authors read and approved the final manuscript.

Conflict of interest

None declared.

References

1. Bokeriya L, Revishvili S, Neminuschy NM. Implantable Cardioverters-Defibrillators in Prevention of Sudden Cardiac Death. *Annals of Arrhythmology*. 2006(4):46-57.
2. Arbolishvili GN, Nasonova SN, Ovchinnikov G. Sudden (Arrhythmic) Death during Holter-monitoring ECG recording. *Cardiac Insufficiency*. 2002;3(4):200.
3. Gilyarov MY, Sulimov V. Heart Rhythm Abnormality Treatment in Subjects with Circulatory Deficiency. *Russian Medical Journal Cardiology*. 2010;22(18):1298-301.
4. Grishaev SL. Myocardial Electrical Instability in Patients Suffered from Ischemic Heart Disease. *Russian Medical Journal*. 2003(2):13-8.
5. Messerii FN, Ventura HO, Elizari DJ, et al. Hypertension and sudden death, increased ventricular ectopic activity in left ventricular hypertrophy. *Amer J Med*. 1984;77:18.
6. Murashko VV, Strutynsky V. *Electrocardiography: Study Guide*. 4th ed. Moscow: MEDpress; 2000. 312 p.
7. Goldstein S, Bayes-de-Luna A, Gumdo-Soldevila J. *Sudden cardiac death*: Armonk: Futura; 1994. 343 p.
8. Orlov VN. *Electrocardiography Guidelines*. 4th edit ed. Moscow: Medical Press Agency; 2004. 528 p.
9. Chen SW. A wavelet-based heart rate variability analysis for the study of nonsustained ventricular tachycardia. *Trans Biomed Eng*. 2002 July 49(7):736-42.
10. Savelieva IV. Stratification of Individuals Suffered from Ventricular Rhythm Disturbance according to Sudden Death Groups. *Cardiology*. 1997(8):82-96.
11. Gottlieb LS, Weisfeldt M, Ouyang P, et al. Silent ischemia as a marker for early unfavorable outcomes in patients with unstable angina. *New Engl J Med*. 1986;314:1214.
12. Shalygin LD, Lyadov KV, Pyatkina TV. Adequate Antiarrhythmic Chronotherapy of IHD Patients. *Cardiology – the XXI century*2001.
13. Gardner PI, Ursel PC, Fenoglio JJ, et al. Electrophysiologic and anatomic basis for fractionated electrograms recorded from healed myocardial infarcts. *Circulation*. 1985;72(3):596-611. PubMed ID: 4017211
14. Bigget JT, Fleisz JL, Kjeiger Rea. The relationships among ventricular arrhythmias, left ventricular dysfunction and mortality in the 2 years after myocardial infarction. *Circulation*. 1984;69:250.
15. Elhendy A, Sozzi FB, van Domburg, et al. Relation between exercise-induced ventricular arrhythmias and myocardial perfusion abnormalities in patients with intermediate pretest probability of coronary artery disease. *Eur J Nucl Med*. 2000 March;27(3):327-32. PubMed ID: 10774886

16. Buxton AE, Kirk MM, Miehaut GT. Current approaches to evaluation and management of patients with ventricular arrhythmias. *Med Health R I* 2001 February;84(2):58-62. PubMed ID: 11272662
17. Kulakowski P, Malik M. Ventricular signal averaged electrocardiography. Risk of Arrhythmia and Sudden Death. London 2001.
18. Rocco MB, Nabel EG, Campbell S, et al. Prognostic significance of myocardial ischemia detected by ambulatory monitoring in patients with stable coronary artery disease. *Circulation*. 1988;78:877.
19. Kleiger RE, Miller JP, Bigger JT, et al. Decreased heart rate variability and its association with increased mortality after acute myocardial infarction. *Amer J Cardiol*. 1987;59:256-62. PubMed ID: 3812275
20. Podrid PJ, Kowey PR. Handbook of cardiac arrhythmia. Baltimore: Williams & Wilkins; 1996. 459 p.
21. Nademanee K, Intarachot V, Josephson Mea. Prognostic significance of silent myocardial ischemia in patients with unstable angina. *J Amer Col Cardiol*. 1987;10(1):1-9. PubMed ID: 3597980
22. Morti V, Bayes-de-Luna A, Arriola J, et al. Value of dynamic QTc in arrhythmology. *New Trends Arrhyth*. 1988;4:683.
23. Kaasik A, Ristimae T, Soopold U, et al. The relationship between left ventricular mass and ventricular late potentials in patients with first myocardial infarction. *J Coronary Artery Disease*. 2001 Oct.;4(1):60.
24. Saeed M, Link MS, Mahapatra S, et al. Analysis of intracardiac electrograms showing monomorphic ventricular tachycardia in patients with implantable cardioverter-defibrillators. *Am J Cardiol*. 2000 Mar 1;85(5):580-7.
25. Cardio-eigenoscop. Useful Model Patent of the Russian Federation. Application No2012134072/14(054263)
26. Nicod H, Polikar R, Petersoh KL. Hypertrophic cardiomyopathy and sudden death. *New Engl J Med*. 1987;316:780.
27. Priori SG, Barhanin J, Hauer R, et al. Genetic and molecular basis of cardiac arrhythmias: impact on clinical management. *Circulation*. 1999 Feb 2;99(4):518-28. PubMed ID: 9927398
28. Myeburg RJ, Spooner PM. Opportunities for sudden death prevention: directions for new clinical and basic research. *Cardiovasc Res*. 2001 May;50(2):177-85. doi: 10.1016/S0008-6363(01)00253-X. PubMed ID: 11334821
29. Ivanov GG, Setnev AS, et al. Main mechanisms, principles of prognosis and prevention of sudden cardiac death. *Cardiology*. 1998(12):64-73.